

# Response of ENSO amplitude to global warming in CESM large ensemble: uncertainty due to internal variability

Xiao-Tong Zheng<sup>1,2,4</sup>  · Chang Hui<sup>1,2</sup> · Sang-Wook Yeh<sup>3</sup>

Received: 3 March 2017 / Accepted: 11 August 2017 / Published online: 21 August 2017  
© Springer-Verlag GmbH Germany 2017

**Abstract** El Niño–Southern Oscillation (ENSO) is the dominant mode of variability in the coupled ocean–atmospheric system. Future projections of ENSO change under global warming are highly uncertain among models. In this study, the effect of internal variability on ENSO amplitude change in future climate projections is investigated based on a 40-member ensemble from the Community Earth System Model Large Ensemble (CESM-LE) project. A large uncertainty is identified among ensemble members due to internal variability. The inter-member diversity is associated with a zonal dipole pattern of sea surface temperature (SST) change in the mean along the equator, which is similar to the second empirical orthogonal function (EOF) mode of tropical Pacific decadal variability (TPDV) in the unforced control simulation. The uncertainty in CESM-LE is comparable in magnitude to that among models of the Coupled Model Intercomparison Project phase 5 (CMIP5), suggesting the contribution of internal variability to the intermodel uncertainty in ENSO amplitude change. However, the causations between changes in ENSO amplitude and the mean state are distinct between CESM-LE and CMIP5 ensemble. The CESM-LE results indicate that a large ensemble of ~15

members is needed to separate the relative contributions to ENSO amplitude change over the twenty-first century between forced response and internal variability.

## 1 Introduction

El Niño–Southern Oscillation (ENSO) is the dominant mode of coupled ocean–atmosphere variability in tropical oceans on interannual timescales, influencing the global climate system. During El Niño (La Niña) events, warm (cold) sea surface temperature (SST) anomalies appear in the eastern equatorial Pacific, tropical convection shifts eastward, and the Walker circulation weakens (intensifies) (Philander 1990). How ENSO responds to global warming is an important issue in climate change sciences (Cai et al. 2015a). Recent studies revealed that the El-Niño induced rainfall variance increases in the eastern and central equatorial Pacific (Power et al. 2013), leading to more frequent occurrences of extreme El Niño and La Niña events (Cai et al. 2014, 2015b), with an eastward shift of ENSO teleconnections over the Pacific and North America (Zhou et al. 2014). This intensification and eastward shift of ENSO-induced atmospheric response results from an El Niño-like warming pattern that most models projects.

Even though the changes in atmospheric characteristics of ENSO are robust, there are still large uncertainties in multimodel ENSO projections. There is no consistent change in ENSO amplitude under global warming among models (Yeh and Kirtman 2007; Guilyardi et al. 2009; Collins et al. 2010; Cai et al. 2015a). The intermodel uncertainty in SST amplitude change is linked to that in the tropical Pacific oceanic warming pattern (Zheng et al. 2016): the El Niño (La Niña)—like warming reduces (increases) the barrier of mean SST to the tropical convection threshold (Johnson and

✉ Xiao-Tong Zheng  
zhengxt@ouc.edu.cn

<sup>1</sup> Physical Oceanography Laboratory/CIMST, Ocean University of China and Qingdao National Laboratory for Marine Science and Technology, Qingdao, China

<sup>2</sup> Key Laboratory of Ocean–Atmosphere Interaction and Climate in Universities of Shandong, Ocean University of China, Qingdao, China

<sup>3</sup> Department of Marine Sciences and Convergent Technology, Hanyang University, Ansan, South Korea

<sup>4</sup> College of Oceanic and Atmospheric Sciences, Ocean University of China, Qingdao 266100, China

Xie 2010), enhancing (weakening) convective feedback on ENSO and further increasing (suppressing) SST variability. Other studies also reported that the intermodel diversity in ENSO amplitude change is related to that in atmospheric feedback (Watanabe et al. 2012; An and Choi 2015; Rashid et al. 2016; Ham and Kug 2016).

However, the model diversity is not the only source for the uncertainty in future climate projections. In fact, the uncertainty in climate prediction/projection results from three distinct sources: model diversity, forcing scenario, and internal variability (Hawkins and Sutton 2009). Among them, internal variability, which is defined as the natural variability of the climate system independent on the external forcing, cannot be neglected for the regional climate projection, especially for the extra-tropical region (Hawkins and Sutton 2009, 2012; Deser et al. 2012a). For example, Deser et al. (2012b) suggested that the internal variability is important for the future projection in North American climate in a 40-member ensemble of climate change simulation. By contrast, the internal variability in tropical region is relative low and the robust mean state change (i.e. 'signal') will emerge in the next few decades (Hawkins and Sutton 2009; Deser et al. 2012a). Nevertheless, it is still unknown that how much internal variability influences regional projections of interannual variability in the tropics, such as ENSO.

The ENSO amplitude shows considerable internal natural variability both in observations and model simulations. Li et al. (2011, 2013) found that ENSO amplitude modulates in the past millennium by using tree-ring records. Such interdecadal modulations of ENSO amplitude impact the global climate via changing atmospheric circulations and teleconnections, including Asia, North America, South America, tropical Pacific and Indian Ocean (Xie et al. 2010b; Chowdary et al. 2012; Li et al. 2013). Based on a long coupled general circulation model (CGCM) simulations, Rodgers et al. (2004) also found significant modulations on interdecadal time scales. Such interdecadal modulation of ENSO amplitude and its relationship with mean state change are investigated extensively by previous studies. (Wittenberg 2002, 2009; Rodgers et al. 2004; Yeh and Kirtman 2004; Fang et al. 2008; Burgman et al. 2008; Sun and Yu 2009; DiNezio et al. 2012; Ogata et al. 2013; Wittenberg et al. 2014). Specifically, the second tropical Pacific decadal variability (TPDV) mode featuring a zonal dipole pattern, is dynamically coupled with ENSO variability in long-term control run with constant forcing (Rodgers et al. 2004; Choi et al. 2013; Ogata et al. 2013). Considering this robust natural interdecadal modulations both in observations and model simulations, the internal variability can potentially change the ENSO amplitude in future climate projections (Stevenson 2012). Therefore, its contribution to uncertainty in ENSO amplitude change under global warming should be evaluated.

In this study, a 40-member large ensemble from Community Earth System Model Large Ensemble (CESM-LE) project is used to investigate the role of internal variability in ENSO response to global warming. It is found that even though the ensemble mean ENSO amplitude increases by 10% with an El Niño-like mean warming in the tropical Pacific, there is a large uncertainty among CESM-LE members. The diversity among ensemble members from the historical run to the RCP8.5 run are associated with that of mean state change, which shows a zonal dipole-like pattern in the tropical Pacific reflecting the second TPDV mode in long-term control run. The uncertainty in CESM-LE is almost comparable with that in a multimodel ensemble from the Coupled Model Intercomparison Project phase 5 (CMIP5). Therefore, a large ensemble is needed for the accurate estimation of forced ENSO response to global warming.

The rest of the paper is organized as follows. Section 2 briefly describes the model datasets and methods used in this study. Section 3 shows ENSO amplitude change in CESM-LE and its relationship with ocean mean warming. In Sect. 4 we compare the uncertainties between CESM-LE and CMIP5 multimodel ensemble. In Sect. 5 we provide a discussion. Section 6 is a summary.

## 2 Data and methods

The CESM-LE project is designed to investigate the climate change in the presence of internal climate variability (Kay et al. 2015). The CESM-LE simulations use the Community Earth System Model, version 1 (CESM1, Hurrell et al. 2013), which consists of coupled atmosphere, ocean, land and sea ice component models. Its horizontal resolution is approximately  $1^\circ$  in all components. The atmospheric component of the model is the version 5 of the Community Atmosphere Model (CAM5) with 30 vertical layers (Neale et al. 2012). The oceanic component of the model is based on the Parallel Ocean Program, version 2 (POP2; Smith et al. 2010) with 60 vertical layers.

In this study, 40 members from CESM1-LE are analyzed to show how internal variability affects ENSO variability in future climate projection. The first ensemble member started from a randomly selected date in the 1850 control simulation with constant preindustrial forcing. Then ensemble member 1 was integrated forward from 1850 to 2100. Ensemble member 2–40 were all started from 1920 to 2100 with slightly different initial conditions. All the CESM-LE members have the same external forcing, which is from the CMIP5 design protocol (Taylor et al. 2012). The model is forced by historical greenhouse gases (GHG), aerosols and other radiative forcing from 1920 to 2005, and representative concentration pathway 8.5 (RCP8.5) forcing from 2006

to 2100, with the radiative forcing reaching  $\sim 8.5 \text{ W m}^{-2}$  near 2100. Since all 40 members use the same model and share the same external forcing scenario, the uncertainty in CESM-LE projections results from internal climate variability alone. To further investigate the role of internal variability, we also analyzed an 1100-year control simulation under constant preindustrial forcing. The detailed information of CESM-LE design can be found in Kay et al. (2015).

To evaluate relative contributions of internal variability and model spread, we used the output of 23 models from the CMIP5 multimodel ensemble organized by the Program for Climate Model Diagnosis and Intercomparison for the Intergovernmental Panel on Climate Change Fifth Assessment Report (Table 1). All of the CMIP5 ensemble members use the same period (1920–2100) and external forcing (historical simulation and RCP8.5 scenario) as CESM-LE. For each model only one ensemble member (r1i1p1) is analyzed in this study, so the multimodel uncertainty in CMIP5 ensemble results both from model differences and from internal variability.

In this study, the SST and rainfall averaged in the eastern equatorial Pacific Niño-3 ( $5^{\circ}\text{S}$ – $5^{\circ}\text{N}$ ,  $90^{\circ}$ – $150^{\circ}\text{W}$ )

region are referred to as the ENSO SST and rainfall indices, respectively. Firstly we remove seasonal cycle in CESM-LE and CMIP5 outputs. Then to focus on the interannual variability, we calculate the anomalies by performing a 3-month running average to reduce intraseasonal variability, and subtracting a 9-year running mean to remove decadal and longer variations. Anomalies in the first 4 years (1920–1923) and last 4 years (2097–2100) were not calculated because the 9-year running mean were not available for those years. We calculated 50-year running standard deviations of ENSO SST and rainfall indices (i.e., years 1925–1974, 1926–1975, so on), and started the analyzed period at the second half of twentieth century (1950–1999). Specifically, the ENSO amplitude ratio between 2046–2095 and 1950–1999 represents the change under global warming quantitatively. We also examined standard deviation of ENSO in 30-year sliding windows, the results of which is very similar to that in 50-year sliding windows.

**Table 1** Twenty-three CMIP5 models used in this study

Model name	Institute (country)
BCC-CSM1-1	Beijing Climate Center, China Meteorological Administration (China)
CanESM2	Canadian Centre for Climate Modeling and Analysis (Canada)
CCSM4	National Center for Atmospheric Research (USA)
CNRM-CM5	Centre National de Recherches Météorologiques (France)
CSIRO-Mk3-6-0	Commonwealth Scientific and Industrial Research Organization in collaboration with the Queensland Climate Change Centre of Excellence (Australia)
FGOALS-g2	State Key Laboratory of Numerical Modeling for Atmospheric Sciences and Geophysical Fluid Dynamics (China)
FGOALS-s2	State Key Laboratory of Numerical Modeling for Atmospheric Sciences and Geophysical Fluid Dynamics (China)
GFDL-CM3	NOAA Geophysical Fluid Dynamics Laboratory (USA)
GFDL-ESM2G	NOAA Geophysical Fluid Dynamics Laboratory (USA)
GFDL-ESM2M	NOAA Geophysical Fluid Dynamics Laboratory (USA)
GISS-E2-R	NASA Goddard Institute for Space Studies (USA)
HadGEM2-CC	Met Office Hadley Centre (UK)
HadGEM2-ES	Met Office Hadley Centre (UK)
INM-CM4	Institute of Numerical Mathematics (Russia)
IPSL-CM5A-LR	L'Institute Pierre-Simon Laplace (France)
IPSL-CM5A-MR	L'Institute Pierre-Simon Laplace (France)
MIROC5	University of Tokyo, Atmosphere and Ocean Research Institute, National Institute for Environmental Studies, and Japan Agency for Marine-Earth Science and Technology (Japan)
MIROC-ESM	University of Tokyo, Japan Agency for Marine-Earth Science and Technology, Atmosphere and Ocean Research Institute, and National Institute for Environmental Studies (Japan)
MIROC-ESM-CHEM	University of Tokyo, Japan Agency for Marine-Earth Science and Technology, Atmosphere and Ocean Research Institute, and National Institute for Environmental Studies (Japan)
MPI-ESM-LR	Max Planck Institute for Meteorology (Germany)
MPI-ESM-MR	Max Planck Institute for Meteorology (Germany)
MRI-CGCM3	Meteorological Research Institute (Japan)
NorESM1-M	Norwegian Climate Centre (Norway)

### 3 ENSO variability change in CESM-LE

ENSO in CESM1 with CAM5 is well simulated and similar to that in the Community Climate System Model, version 4 (CCSM4), even though the magnitude is overestimated (Hurrell et al. 2013). Figure 1 shows monthly standard deviation of Niño-3 SST in observations (1950–1999) based

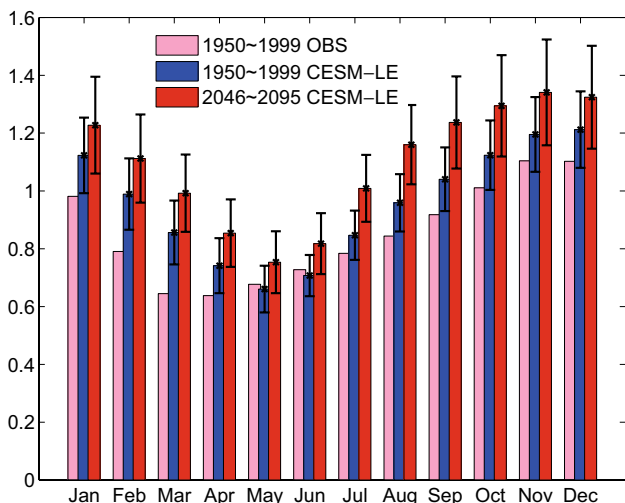
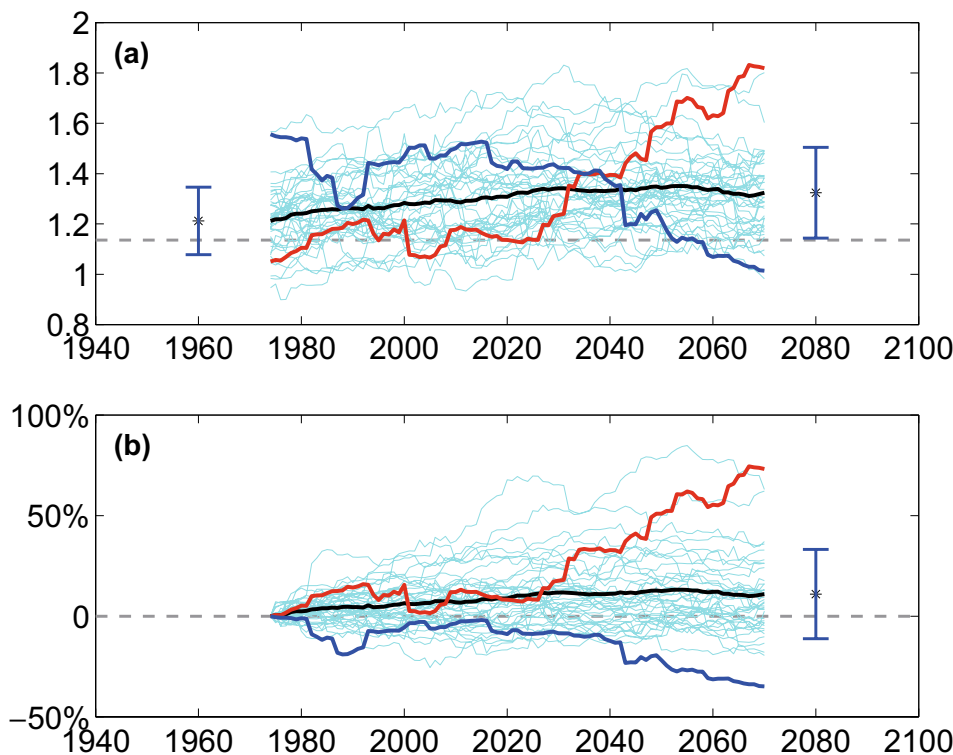


**Fig. 1** Monthly standard deviations of Niño-3 index in observations during 1950–1999 (pink bars), CESM-LE ensemble mean during 1950–1999 (blue bars) and 2046–2095 (red bars). The error bars denote the standard deviation of inter-member variability

**Fig. 2** 50-year running time series of **a** Niño-3 SST variance and **b** its percentage change relative to the period 1950–1999. The black thick line denotes the multi-member ensemble mean. The red and blue lines denote the ensemble member with most increased (ensemble member 5) and decreased (ensemble member 20) ENSO variability. The error bars are the standard deviations of inter-member variability during 1950–1999 (left) and 2046–2095 (right), respectively. The years shown on the x-axis denote the 25th year of the 50-year period



on the National Oceanic and Atmospheric Administration Extended Reconstructed SST version 3b dataset (Smith et al. 2008), with that for the periods before (1950–1999) and after (2046–2095) the GHG-induced warming in CESM-LE. As in observations, the peak of SST variance appears during boreal winter in both periods. Unless mentioned otherwise, we use averaged Niño-3 indices of SST and rainfall during November–December–January in this study.

#### 3.1 ENSO amplitude change and its uncertainty

The ensemble mean ENSO amplitude increases under global warming in CESM-LE with large inter-member uncertainty. Figure 2a shows CESM-LE ENSO variance in the 50-year sliding windows, starting at 1950–1999. The ensemble mean ENSO amplitude increases from 1.21 °C (1950–1999) to 1.32 °C (2046–2095), with large inter-member diversity throughout the simulation. For the period 1950–1999, ENSO amplitude ranges from 0.95 to 1.56 °C, while from 1.0 to 1.8 °C during 2046–2095. With an increase by 10.7% in the ensemble mean, ENSO amplitude projection shows a much larger diversity among ensemble members (Fig. 2b), ranging from –34.6% (ensemble member 20) to 72.7% (ensemble member 5). The inter-member standard deviation is 22.8% and more than twice ensemble mean value, indicating that the internal variability is one of the main source of uncertainty in future projections of ENSO variability.

The increased ENSO amplitude with large uncertainty in CESM-LE is also demonstrated in Fig. 3 (the left columns). The SST amplitude change are highly correlated with that of rainfall at  $r=0.88$  (not shown). A member with enhanced (weakened) SST amplitude of ENSO usually shows an enhanced (weakened) atmospheric response represented by rainfall amplitude, reflecting that the Bjerknes (1969) feedback is efficiently working in the tropical Pacific in CESM-LE. Compared with SST variability, the amplitude in Niño-3 rainfall shows a significant increase by 67.4% in the ensemble mean, in spite of an even larger inter-member diversity (Fig. 3b). This increased ENSO rainfall variability

is associated with the warming pattern in the tropical Pacific (Power et al. 2013; Cai et al. 2014; Zheng et al. 2016). Similar to most model projections, CESM-LE shows an El Niño-like warming pattern in the tropical Pacific (Fig. 4), with reduced evaporative damping on the equator, weakened Walker circulation and associated oceanic dynamical response (Liu et al. 2005, 2016; Vecchi and Soden 2007; Xie et al. 2010a; Lu and Zhao 2012; Luo et al. 2015). This El Niño-like warming pattern reduces the barrier of mean SST to the tropical convection threshold in the eastern equatorial Pacific, strengthens the convective feedback, and further amplifies the ENSO variability via the Bjerknes feedback. Indeed, the model uncertainty in ENSO amplitude change is associated with the warming pattern in the tropical Pacific (Watanabe et al. 2012; Zheng et al. 2016). Next we examine the relationship between changes in ENSO variability and mean state among CESM-LE members.

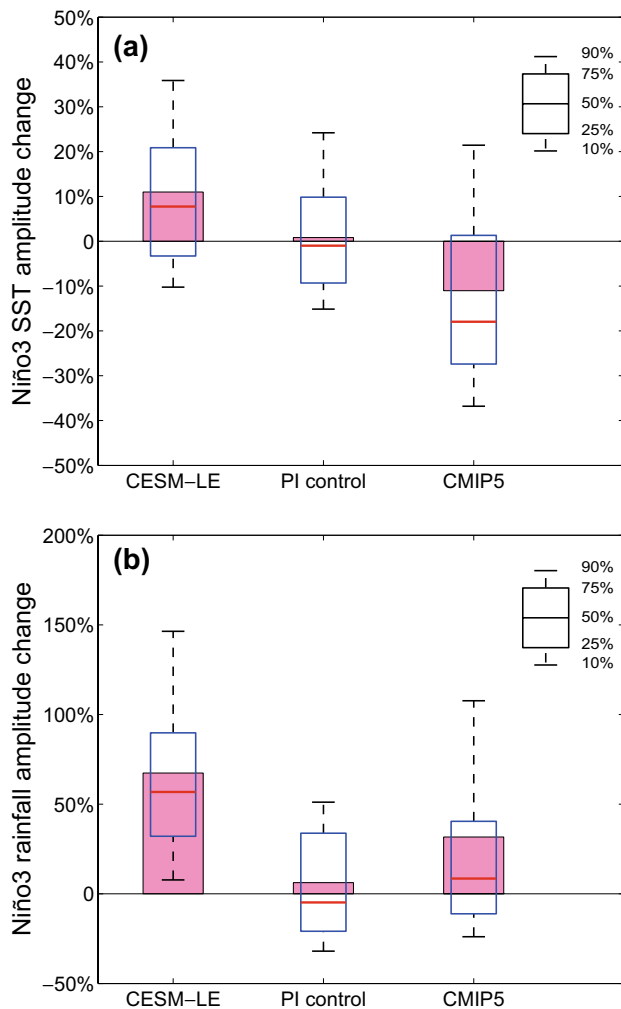


**Fig. 3** The multi-member ensemble mean percentage changes between 2046–2095 and 1950–1999 in Niño-3 **a** SST and **b** rainfall standard deviations in CESM-LE (left) and CMIP5 models (right). The box-and-whisker plots show the 10th, 25th, 50th, 75th, and 90th percentiles, representing the inter-member variability. The middle column shows the ensemble mean with inter-member variability of 100 ENSO amplitude differences between the first and last 50-year windows of randomly selected 145-year segment in 1100-year unforced control run

### 3.2 The relationship with the mean state change

Different from the CMIP5 ensemble [see Fig. 3 in Zheng et al. (2016)], the warming patterns in CESM-LE ensemble members are quite similar. All of them show an El Niño-like warming pattern in the tropical Pacific, highly spatially correlated with the ensemble mean (Fig. 4). To extract the slight diversity of these warming patterns associated with the internal variability, we performed an inter-member empirical orthogonal function (EOF) on the mean SST warming following our previous study (Zheng et al. 2016). The leading mode explaining nearly half of the total variance shows an east–west dipole pattern in the tropical Pacific (Fig. 5a). A member with a positive principal component (PC) value shows a more (less) warming in the eastern (western) tropical Pacific, and vice versa. We found that PC1 is highly correlated with the inter-member diversity in ENSO SST amplitude changes ( $r=0.91$ ) (Fig. 6a), indicating a close relationship with the ocean mean warming. Additionally, PC1 is correlated with the inter-member diversity in ENSO rainfall amplitude change at  $r=0.76$  (Fig. 6b).

To further illustrate the relationship with mean state change in CESM-LE, here we selected two representative members, ensemble member 5 and 20, with the most increased and decreased ENSO amplitude, respectively. For the mean state change, ensemble member 5 shows a more zonal gradient and significant positive PC1 value, while ensemble member 20 shows a roughly uniform warming along the equator with the largest negative PC1 value (Figs. 4, 5). Consequently, in ensemble member 5 with a more pronounced zonal warming gradient, the ENSO-induced rainfall and zonal wind anomalies increase and shift eastward along the equator, reflecting the enhanced atmospheric feedback (Fig. 7a, b). By contrast, rainfall and zonal

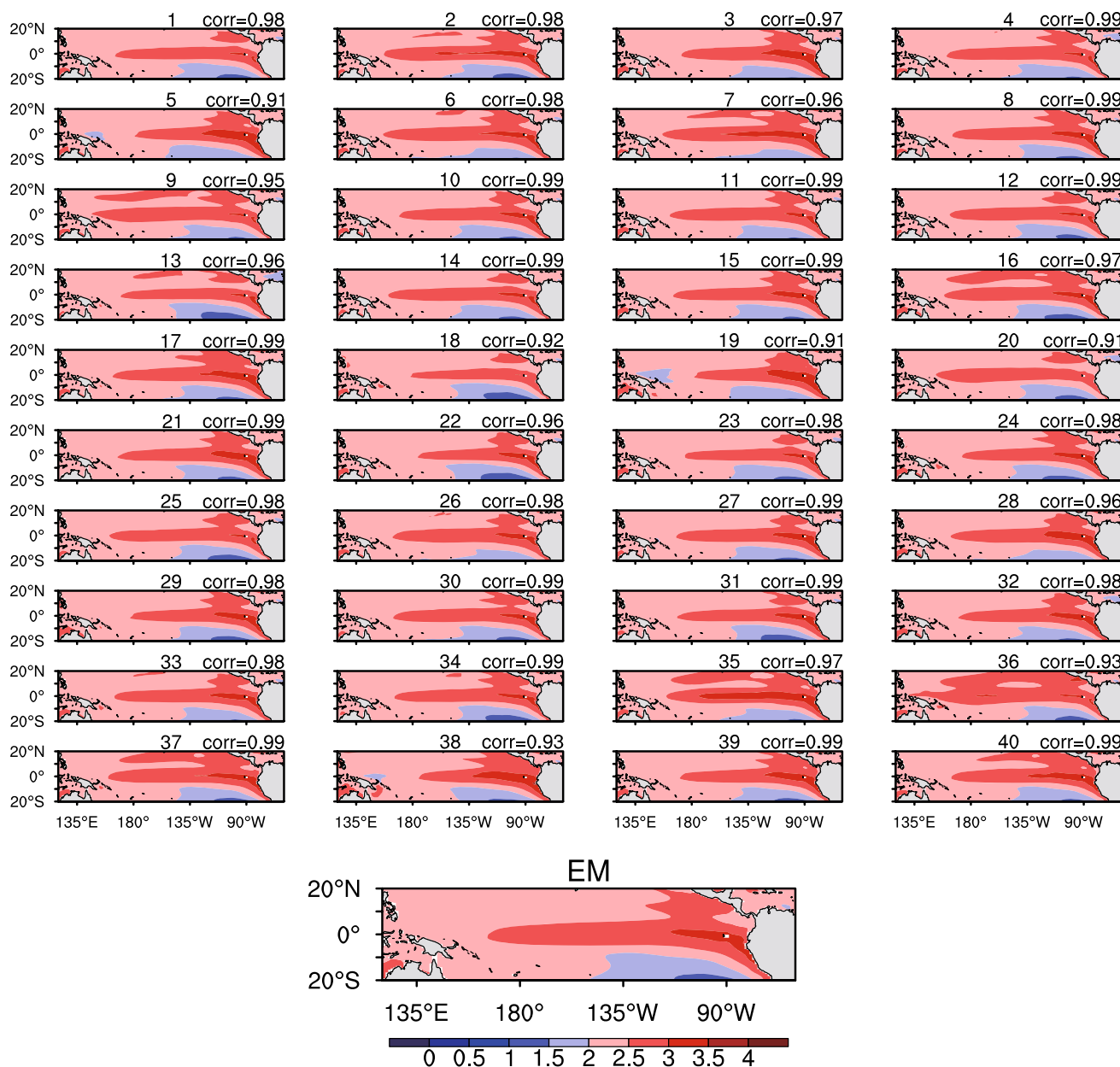


**Fig. 4** SST changes (°C) between 2046–2095 and 1950–1999 under global warming for 40 members of CESM-LE and ensemble mean (*bottom*) in the tropical Pacific. The *values at the top right* of each panel are the spatial correlations of warming pattern with that of ensemble mean

wind anomalies even shift westward in ensemble member 20 (Fig. 7c, d).

Derived from internal variability, the first inter-member EOF mode of ocean mean warming is similar to a natural TPDV mode in the long-term control run with constant CO<sub>2</sub> forcing, which also displays an east–west zonal dipole pattern in SST and covaries with interdecadal ENSO variability (Rodgers et al. 2004; Yeh and Kirtman 2004; Choi et al. 2013; Ogata et al. 2013). Here we performed the EOF analysis on the 11-year low-passed SST anomalies in the tropical Pacific based on the 1100-year CESM1 preindustrial

control run (Fig. 8). Consistent with previous studies (Choi et al. 2013; Ogata et al. 2013), the first mode shows an El Niño-like decadal variability, while the second mode shows an east–west dipole-like pattern, explaining nearly 24% of the variance. The PC2 is correlated with 11-year running variance of Niño-3 index at  $r=0.68$ , above the 95% significance level, indicating the second mode is associated with the natural decadal modulation of ENSO amplitude. In addition, this mode is highly spatially correlated with the first inter-member EOF mode of SST warming (see Fig. 5a) at  $r=0.95$ , corroborating this relationship.

**Fig. 5** **a** The first EOF mode of inter-member spread in SST change between 2046–2095 and 1950–1999 in CESM-LE. **b** The inter-member principal component of first mode

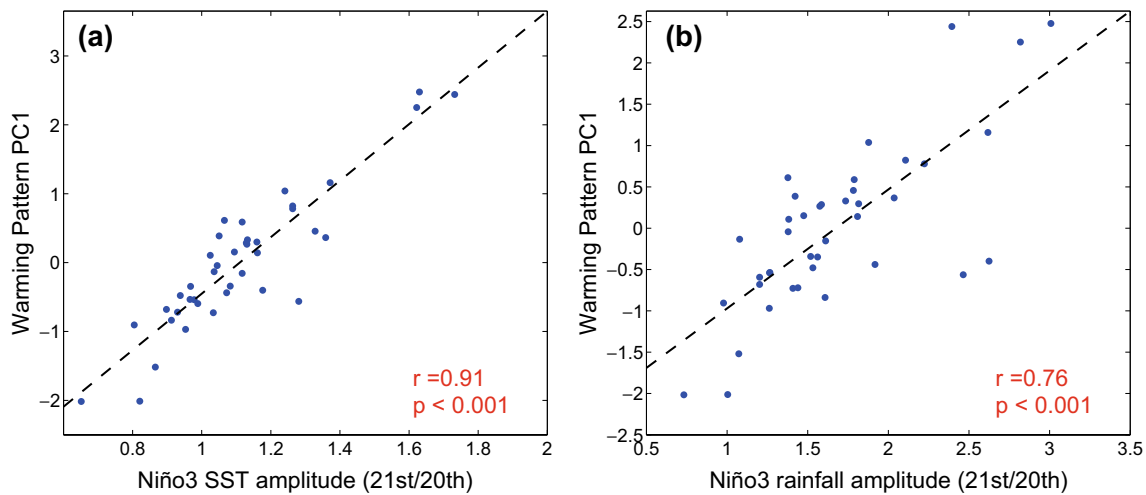
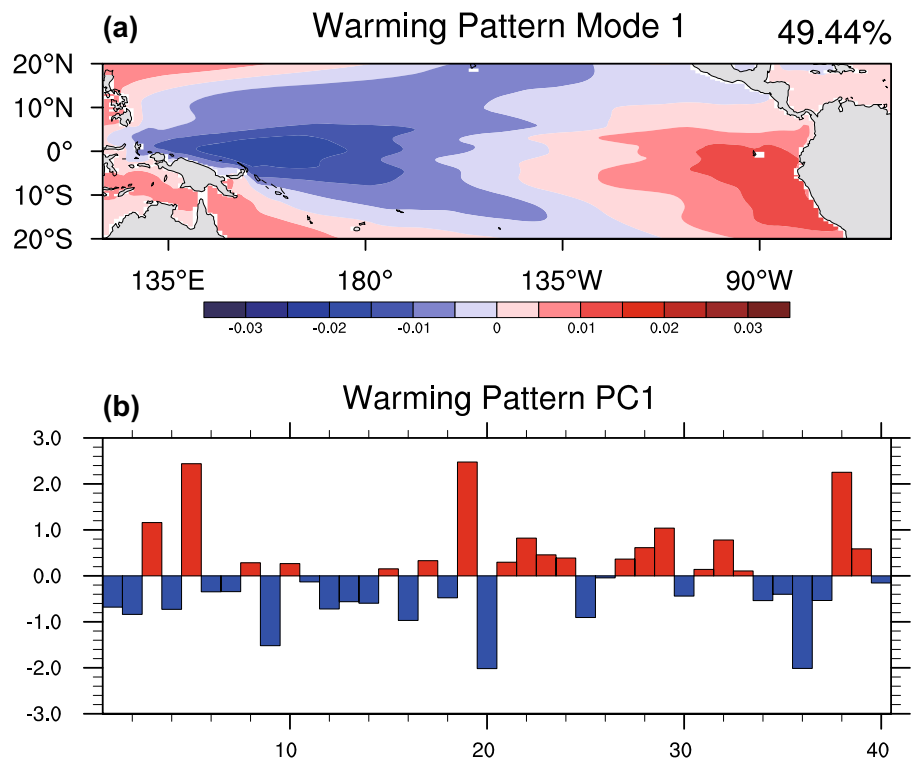


**Fig. 6** The scatterplots of PC1 for inter-member SST spread in CESM-LE with the 21st to twentieth century ratio of standard deviation for Niño-3 **a** SST and **b** rainfall. The dashed line denotes the linear regression

To further illustrate the contribution of internal variability, we calculated a total of 100 differences of ENSO amplitude between the first and last 50-year windows of randomly selected 145-year segment in 1100-year unforced control run, such as differences between years 106–155 and 11–60 and so on. The range of ENSO amplitude in control run (the box-and-whisker plot of the middle column in Fig. 3a) is comparable to that in CESM-LE. By contrast, the uncertainty in ENSO rainfall amplitude becomes larger in CESM-LE than that in control run (Fig. 3b), indicating the

intensified ENSO-induced rainfall anomalies under global warming.

#### 4 Comparison to CMIP5 multimodel ensemble

Previous studies usually used CMIP5 multimodel ensemble to investigate the ENSO amplitude change in future climate projections (Watanabe et al. 2012; Cai et al. 2014; Ham and Kug 2016; Zheng et al. 2016). However, most of them used

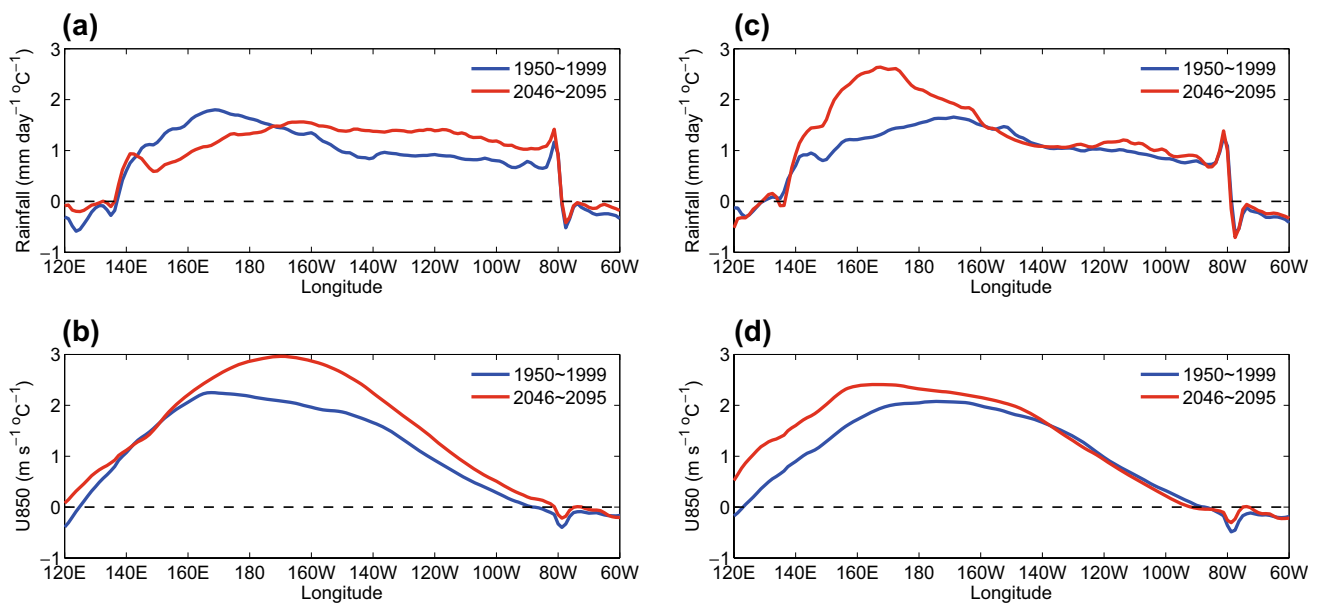


**Fig. 7** The **a** rainfall ( $\text{mm day}^{-1}$ ) and **b** zonal wind ( $\text{m s}^{-1}$ ) regression along the equator (averaged in  $5^{\circ}\text{S}$ – $5^{\circ}\text{N}$ ) upon Niño-3 SST anomalies during NDJ in CESM-LE member 5. **c**, **d** same as **a**, **b** but in member 20

only one ensemble member for individual models. Therefore, model spread results both from model diversity and internal variability, while uncertainty in CESM-LE is from internal variability alone. Comparing CESM-LE and CMIP5 ensemble can help us understand the relative importance of the two factors to uncertainty in the multimodel ensemble.

In this study, we collected 23 CMIP5 models with a single ensemble member. ENSO amplitude in CMIP5 ensemble decreases slightly by about 10% with a large diversity among models (Fig. 9). The relative change of ENSO amplitude ranges from  $-52.5\%$  in FGOALS-g2 to  $+72.4\%$  in MRI-CGCM3 in 2045–2095. The standard deviation of inter-model variability is 28.6% in CMIP5, 1.2 times of that in CESM-LE. Overall, the uncertainty among CESM-LE members is comparable with the CMIP5 model spread (the box-and-whisker plot of the right column in Fig. 3a), indicating internal variability being an important source of uncertainty in ENSO projections under global warming.

Similar results are shown in the scatter diagrams of Niño-3 SST amplitude during 1950–1999 and 2046–2095 (Fig. 10). In a warmer climate, the ensemble mean value of ENSO amplitude increases in CESM-LE while decreases slightly in CMIP5 ensemble. It is conceivable that the fluctuation range in ENSO amplitude in CESM-LE, which is derived from a same model, is smaller than that in CMIP5 ensemble both under present-day and future climates (horizontal and vertical error bars in Fig. 10, respectively). However, the spread in ENSO amplitude change, which is represented by the radius of circle around the ensemble mean, are almost same in CESM-LE and CMIP5 ensemble, suggesting

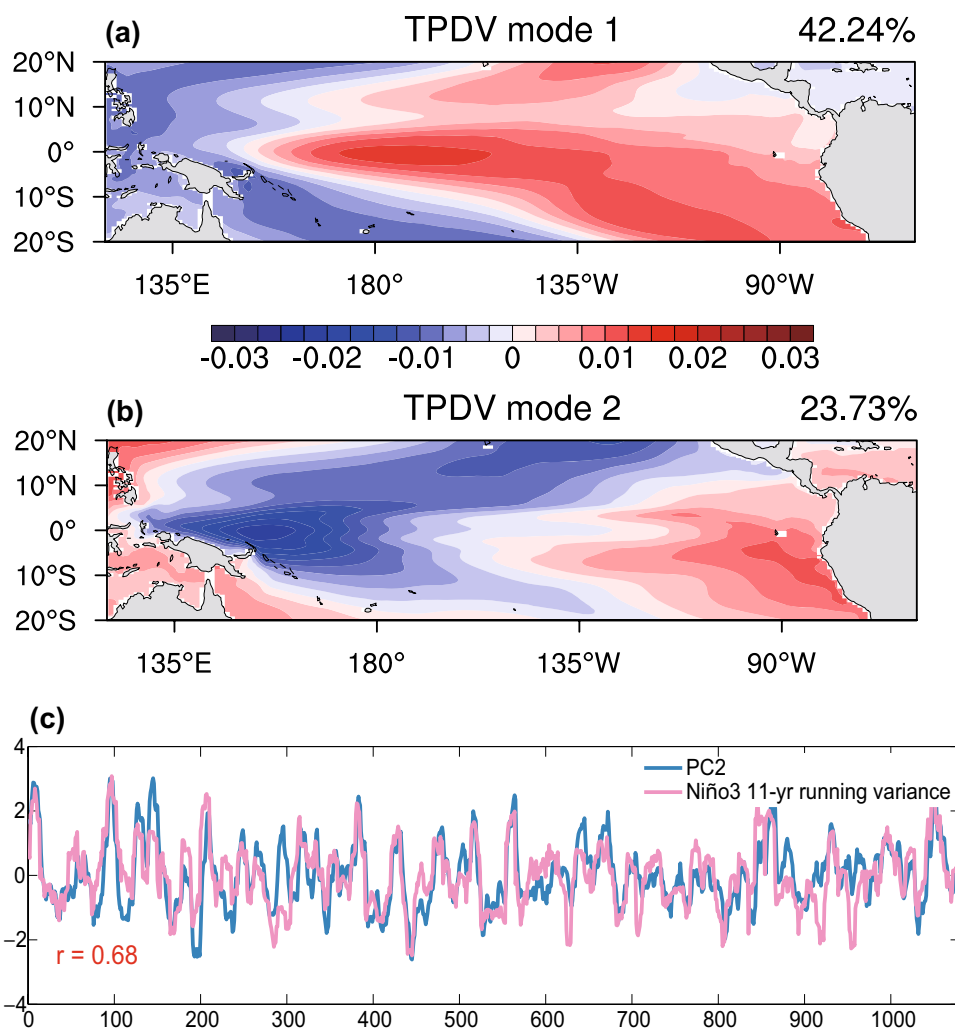
that the interference effect by internal variability cannot be ignored on detecting ENSO response to global warming.

The intermodel diversity of ENSO amplitude is also related to that in mean ocean warming pattern among CMIP5 models. Here we examine the regression of ocean mean warming in tropical Pacific upon ENSO amplitude change to further compare the relationships between changes in mean state and ENSO amplitude in CESM-LE and CMIP5. The regression map in CESM-LE shows the zonal dipole-like pattern, quite similar to the first inter-member EOF mode of mean SST warming (Fig. 11a). By contrast, for CMIP5 models, the associated warming pattern shows enhanced warming in the eastern equatorial Pacific (Fig. 11b).

In CMIP5 ensemble, our previous study suggested that mean warming pattern is considered to change the ENSO amplitude via regulating the convective feedback (Zheng et al. 2016). To show this effect of ocean warming pattern on tropical convection, here we define the relative SST in Niño-3 region ( $T_{\text{Niño-3}}^*$ ) as  $T_{\text{Niño-3}}^* = T_{\text{Niño-3}} - T_{\text{tropical-mean}}$  following Zheng et al. (2016), where  $T_{\text{Niño-3}}^*$  is SST in the Niño-3 region and  $T_{\text{tropical-mean}}$  is the tropical mean SST over  $20^{\circ}\text{S}$ – $20^{\circ}\text{N}$ . The relative SST change ( $\Delta T_{\text{Niño-3}}^*$ ) between 2046–2095 and 1950–1999, which is a good indicator for the warming pattern in the tropical Pacific, is significantly correlated with amplitude changes in ENSO SST and rainfall among CMIP5 models (Fig. 12a, b). The increased ENSO amplitude in CESM-LE ensemble mean also reflects this explanation: An El Niño-like warming pattern (Fig. 4) reduces the barrier to deep convection in the eastern equatorial Pacific, intensifies the convective feedback and ENSO



**Fig. 8** Spatial SST pattern for **a** first TPDV and **b** second TPDV mode in 1100-year CESM1 control run. **c** The PC of second TPDV mode (blue line) and 11-year sliding standard deviation of Niño-3 index (pink line)



variability. As a result, ensemble mean Niño-3 SST and rainfall amplitudes both increase in CESM1 future projection.

Additionally, ENSO amplitude can also be modulated substantially by changes in zonal gradient of equatorial SST through strengthening air–sea coupling (An and Choi 2015). To testify this mechanism, we define a zonal SST gradient index represented by the difference between eastern (110°–80°W, 10°S–10°N) and western (140°E–180°, 10°S–10°N) equatorial Pacific. The intermodel diversity of change in zonal SST gradient index is also significantly correlated to that in ENSO amplitude at  $r = 0.51$  (Fig. 13a). These results suggest that changes in  $T_{\text{Niño-3}}^*$  (i.e. local convective feedback) and zonal SST gradient both contribute to modulating ENSO activity.

By contrast, in CESM-LE the change in ENSO amplitude is only highly correlated with that in zonal SST gradient (Fig. 13c, d), but shows weak relationship with  $\Delta T_{\text{Niño-3}}^*$  (i.e. local convection, Fig. 12c, d). We also found that the PC of second TPDV mode, which is correlated with the ENSO amplitude modulation, shows no significant correlation with

11-year running  $T_{\text{Niño-3}}^*$  in 1100-year control run ( $r = 0.17$ , not shown). The weak correlation between changes in local convection and zonal SST gradient can also be found among CMIP5 models (Fig. 13b). On the other hand, the PC of first TPDV mode, which shows an El Niño-like pattern, is highly correlated with 11-year running  $T_{\text{Niño-3}}^*$  ( $r = 0.83$ ). However, the first TPDV mode only weakly correlated with ENSO amplitude modulation at  $r = 0.28$  (not shown), indicating that the pattern of first TPDV mode cannot regulate ENSO amplitude via convective feedback. Indeed, different to the warming pattern in CESM-LE (Fig. 4), the first TPDV mode shows a basin-wide warming. Its maximum warming even locates in the central to western equatorial Pacific (Fig. 8a). This pattern is unfavorable to attracting rainfall eastward and strengthening ENSO activity (An and Choi 2015).

It is also worth noting that the warming patterns in CMIP5 (see Fig. 3 in Zheng et al. 2016) are much more divergent than that in CESM-LE, which all display an El Niño-like pattern with weakened zonal SST gradient (Fig. 4). Therefore, diversities in  $\Delta T_{\text{Niño-3}}^*$  (horizontal

**Fig. 9** As in Fig. 2 but for 23 CMIP5 models. The red and blue lines denote the model with most increased (MRI-CGCM3) and decreased (FGOALS-g2) ENSO variability. The years shown on the x-axis denote the 25th year of the 50-year period

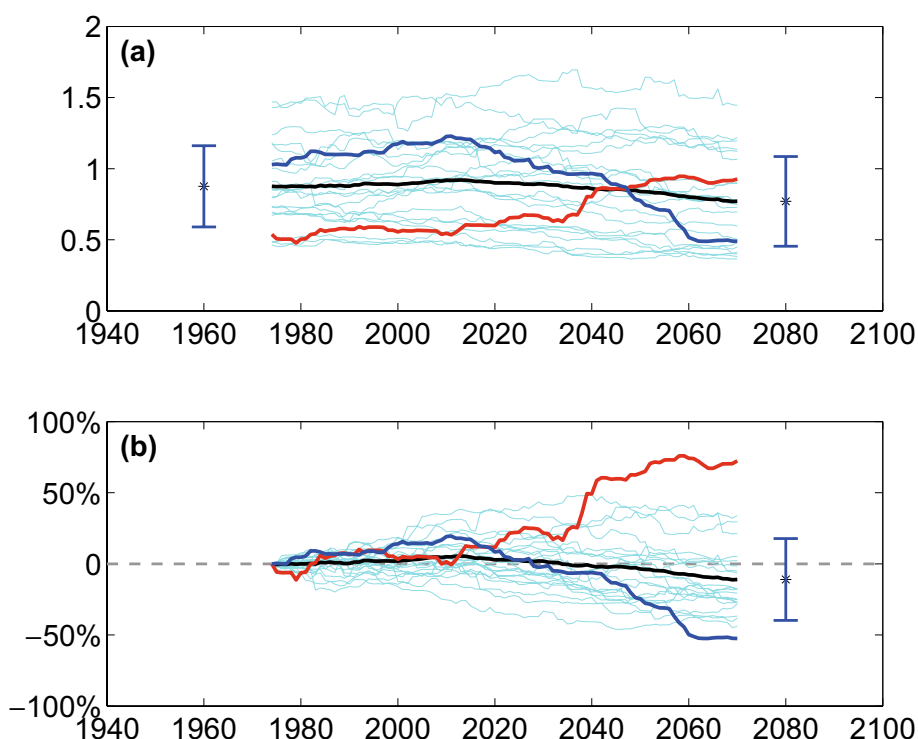
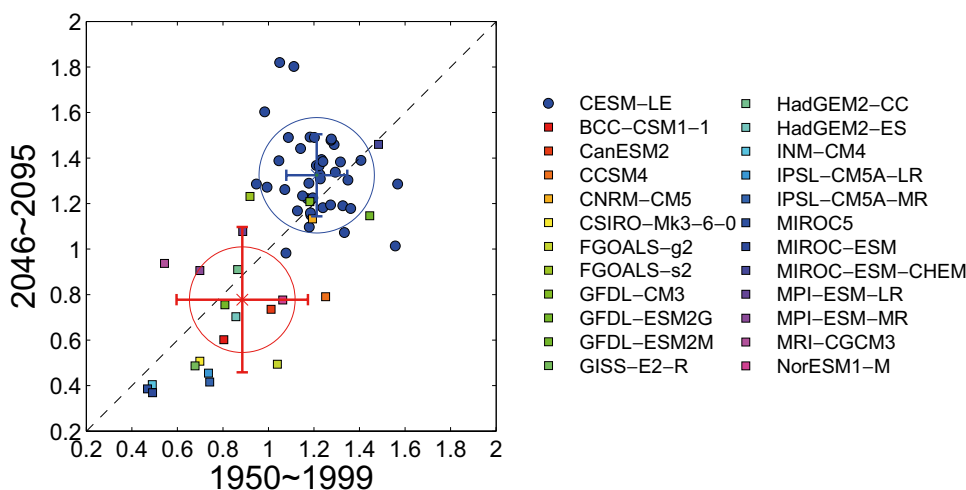


**Fig. 10** Scatterplots of standard deviation of Niño-3 SST for NDJ between 1950–1999 and 2046–2095. Blue dots denote values derived from CESM-LE and squares denote values derived from CMIP5 models. The blue (red) asterisks and error bars denote the ensemble mean and inter-member (intermodel) standard deviation. The radius of circle around the ensemble mean denotes the inter-member (inter-model) standard deviation of 2046–2095 minus 1950–1999 differences



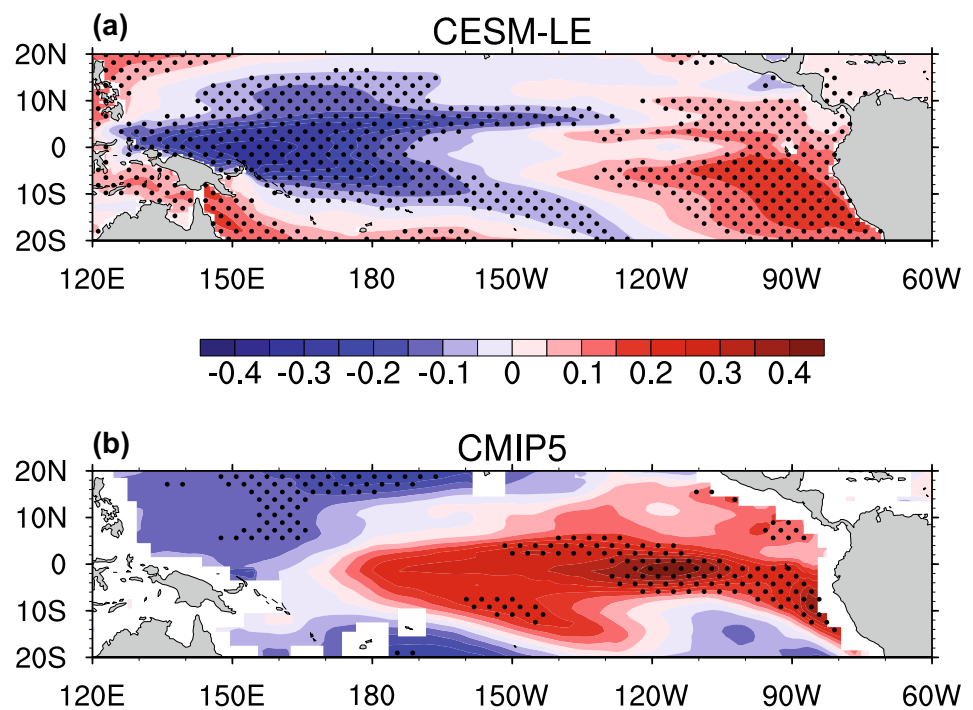
error bars in Fig. 12a, b) and changes in zonal SST gradient index (horizontal error bars in Fig. 13a, b) are both much smaller among CESM-LE members than those among CMIP5 models. By contrast, the amplitude uncertainty in CESM-LE reaches 80% of that in CMIP5, suggesting this large spread in ENSO amplitude change may not be caused by the slight mean state diversity. These results imply the distinct causations between ENSO response and ocean warming pattern in CESM-LE and CMIP5 ensemble, which will be discussed in the next section.

## 5 Discussion

### 5.1 Detecting the significance of ENSO amplitude change

Considering the relative large uncertainty due to internal variability, the significance of ENSO response in ensemble mean need to be detected. We evaluate the 95% statistical significance of the ensemble mean changes against a null hypothesis of zero change using a 2-sided Student's *t* test

**Fig. 11** The regression of inter-member spread in SST change upon ENSO amplitude change between 2046–2095 and 1950–1999 in **a** CESM-LE and **b** CMIP5 ensemble. Grid points marked with filled dots exceed the 95% confidence level based on Student's *t* test



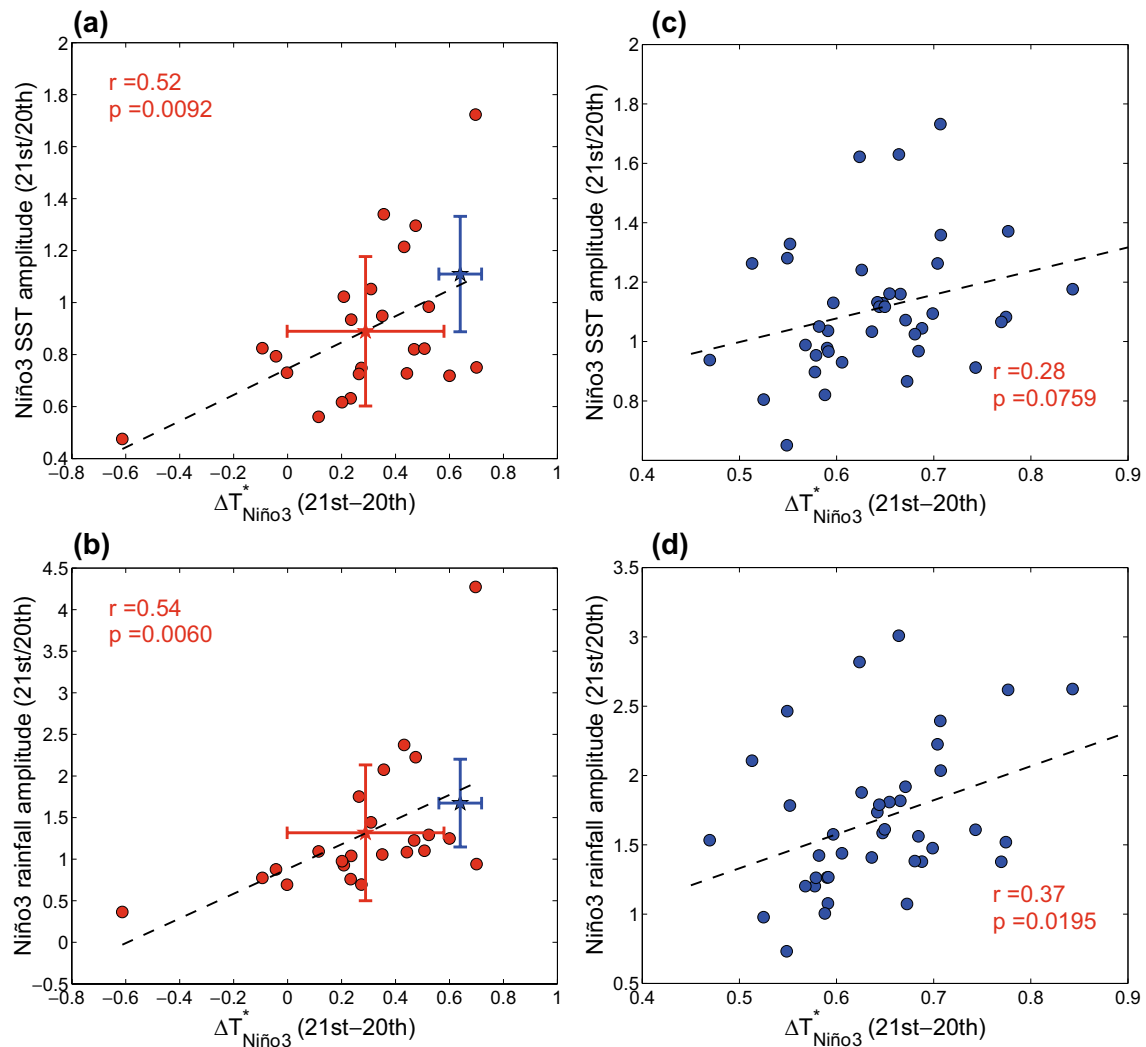
(1-sided *t* test for SST change), which is modified from Deser et al. (2012a). The minimum number of ensemble members ( $N_{min}$ ) needed to detect the forced response represented by ensemble mean at the 95% significance level is then calculated. Here the  $N_{min}$  is a measure of the amplitude of the forced signal (ensemble mean) relative to the noise (ensemble member spread). The detailed information of the test method can be found in the appendix.

Figure 14 shows the 50-year running mean of changes in Niño-3 SST,  $T_{Ni\tilde{3}}^*$ , and zonal SST gradient index in ensemble mean and individual members (right axis), along with the associated  $N_{min}$  time series (left axis). Both in CESM-LE and CMIP5, a significant change in  $T_{Ni\tilde{3}}$  is detected with a single member at the beginning of the twenty-first century due to strong radiative forcing in RCP8.5 scenario. Additionally, changes in  $T_{Ni\tilde{3}}^*$  and zonal SST gradient index is also significant after ~2030 with 1–2 members in CESM-LE on account of an El Niño-like warming pattern in all ensemble members (Fig. 4). By contrast, changes in  $T_{Ni\tilde{3}}^*$  and change in zonal SST gradient index in CMIP5 are significant with more ensemble member because of considerable intermodel variation of tropical SST warming pattern (Zheng et al. 2016). An ensemble of 2–4 (4–6) models is still needed to detect the forced response of  $T_{Ni\tilde{3}}^*$  (zonal SST gradient index) after 2000. In sum, the mean SST change in the tropical Pacific is significant both in CESM-LE and CMIP5, and shows relative large signal-to-noise ratio (Hawkins and Sutton 2012; Deser et al. 2012a).

By contrast, the significant signal of ENSO response emerges much later than ocean mean warming (Fig. 15a).

In CESM-LE, even though ensemble mean ENSO amplitude increases relative to the period 1950–1999, the relatively large number of ensemble member (~15) is still needed to detect it. Note that the  $N_{min}$  decreases to less than 10 in the window centered at ~2030, and then increases gradually. This reflects a non-unidirectional response of ENSO amplitude to anthropogenic forcing (Kim et al. 2014). Furthermore, it shows no significant ENSO response throughout the twenty-first century with slight decrease in CMIP5 ensemble mean (Fig. 15c). Thus robust change in ENSO variability can hardly be detected due to smaller signal-to-noise ratio. Even only considering the uncertainty due to internal variability in CESM-LE, a relative large number of ensemble members (~15) are needed to detect the forced response.

It should be noted that the significance calculation is sensitive to the selected present-day climate. Indeed, if we calculate change relative to first 50-year window in period 1925–1974, a significant response in ENSO variability can be detected after 1980s with an ensemble of 3–6 members in CESM-LE (Fig. 15b). The significant signal is related to the rapid increase in ENSO amplitude during the mid-twentieth century, which is consistent with observations (Chowdary et al. 2012). However, this remarkable ENSO intensification seems not to be forced by GHG increase (note that the magnitude in global warming is relatively small in the twentieth century). We suggest that the ENSO intensification might be attributed to the nearly same initial oceanic condition at 1920 shared by all CESM-LE members. Indeed, compared with the climatology in preindustrial control run, NDJ SST in 1920 shows an evident cooling in the eastern equatorial



**Fig. 12** Inter-model *scatterplots* between  $\Delta T_{\text{Niño-3}}^*$  ( $^{\circ}\text{C}$ ) and the twenty-first to twentieth century ratio of standard deviation for Niño-3 **a** SST and **b** rainfall in CMIP5 ensemble. **c**, **d** As in **a**, **b** but for CESM-LE. The red and blue asterisks and error bars denote

the ensemble mean and inter-member standard deviations in CMIP5 ensemble and CESM-LE, respectively. The *dashed line* denotes the linear regression. The years shown on the *x-axis* denote the 25th year of the 50-year period

Pacific in most members (not shown), in favor of suppressing ENSO activity. By contrast, with a stochastic present-day climate, the ensemble mean change in CMIP5 remains insignificant under global warming relative to the period 1925–1974 (Fig. 15d).

## 5.2 The causations between ocean mean warming and ENSO amplitude change

Though the ENSO responses to global warming in both CESM-LE and CMIP5 are associated with ocean mean warming, the casual relationships are distinct in CESM-LE and CMIP5. In CMIP5 models, the mean warming pattern, which emerges earlier, is first forced by radiative forcing, and then affects the ENSO variability via regulating the

air-sea coupling (An and Choi 2015; Zheng et al. 2016). However, the mechanism of ENSO natural modulation is still being debatable: several studies suggested the effect of low-frequency variability to ENSO amplitude (Wittenberg 2002; Fang et al. 2008; DiNezio et al. 2012), while others suggested the interaction between ENSO modulation and decadal internal variability, pointing out ENSO's nonlinearity is important to the mean state change (Rodgers et al. 2004; Watanabe and Wittenberg 2012; Ogata et al. 2013; Wittenberg et al. 2014). Therefore, the ENSO amplitude change due to internal variability may not simply result from the mean state change. Here our results suggest the latter mechanism may works on the uncertainty due to internal variability. Slight differences of mean warming among CESM-LE members are not adequate to affecting ENSO

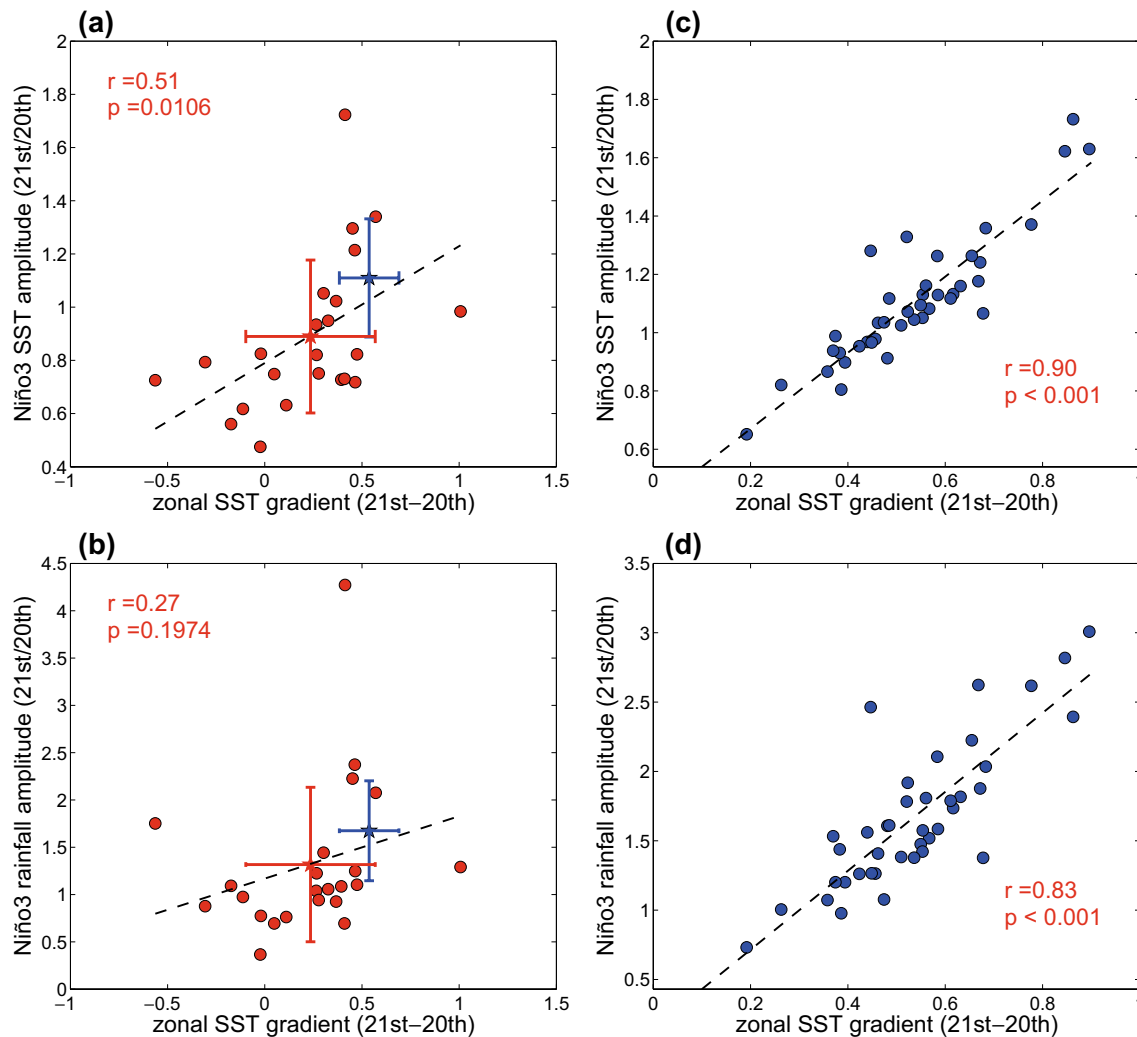


**Fig. 13** As in Fig. 11 but for changes in zonal SST gradient index

variability via changing convective feedback effectively as in CMIP5 (Figs. 12, 13), but may result from the rectification of internal ENSO amplitude modulation. Similarly, uncertainty in ENSO amplitude change in CESM-LE results from interaction between chaotic ENSO perturbation and TPDV, and is not predictable in coupled model projections (Wittenberg et al. 2014). In this case, the magnitude in ENSO amplitude change is largely affected by the random ENSO activity in present-day climate. Indeed, the inter-member correlation between ENSO amplitude in present-day climate (1950–1999) and ENSO amplitude change under global warming is significantly correlated at  $r = -0.72$  (not shown). As a circumstantial evidence, the ensemble mean change relative to the first 50-year window of period 1925–1974 is more significant, which is restricted by the nearly same initial oceanic condition for all ensemble members (Fig. 15c).

It should be noted that the ENSO-induced TPDV is largely affected by the performance of model to simulate

ENSO variability: models with a large (small) ENSO amplitude simulate strong (weak) interaction between ENSO and mean state, leading to intensified (reduced) dipole-like TPDV mode (Choi et al. 2013). Because of the excessively strong ENSO amplitude compared with observations and other CMIP5 models (Figs. 1, 10), the effect of internal variability on ENSO amplitude might be overestimated in CESM-LE. If available, we will use large ensemble from other models with more realistic ENSO simulation to evaluate uncertainty in ENSO response to global warming due to internal variability in the future.

## 6 Summary

Internal variability is an important component of uncertainty in future climate projections. In this study, a 40-member large ensemble from CESM-LE project is analyzed to assess

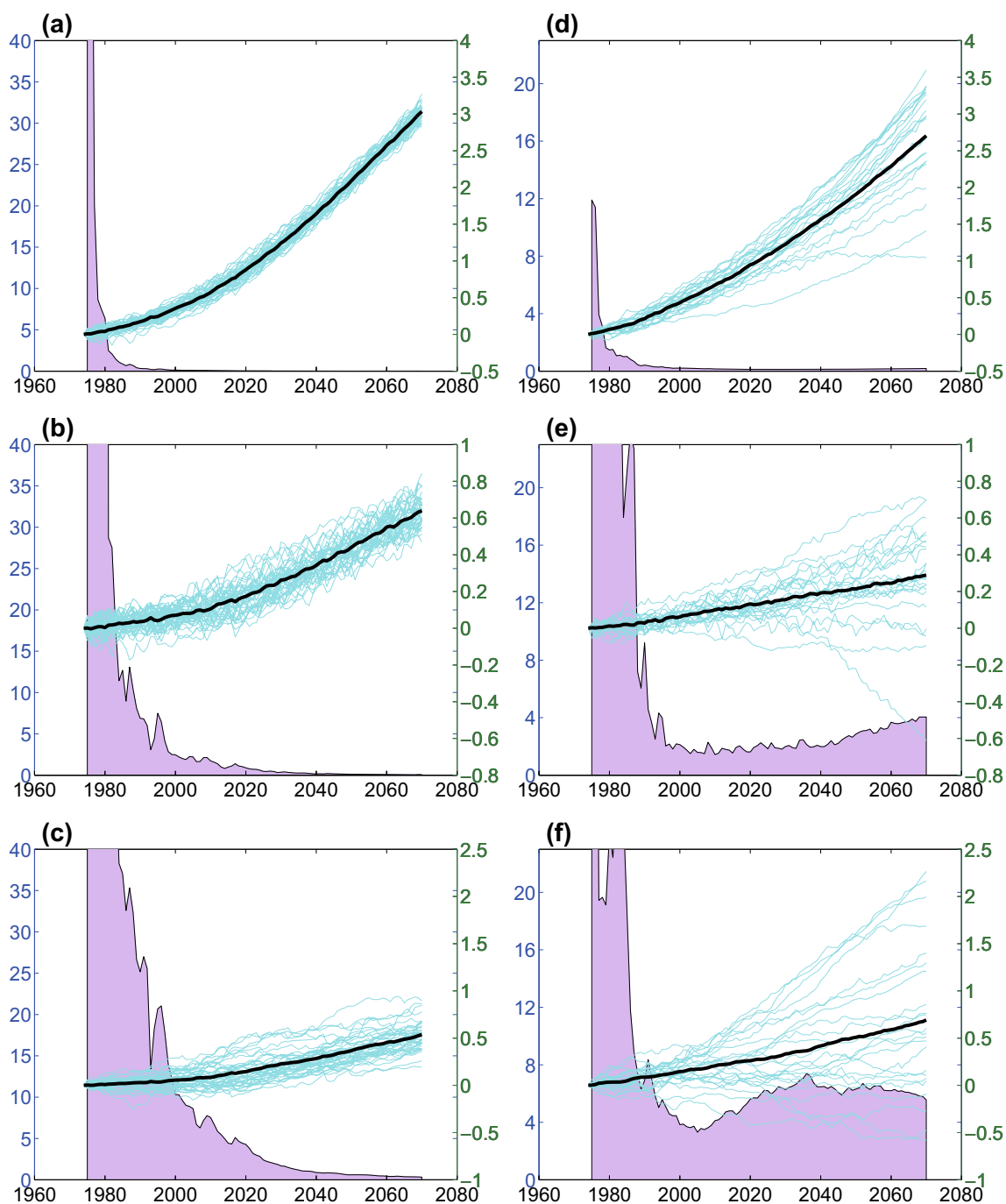


**Fig. 14** 50-year running mean NDJ time series of **a** Niño-3 SST, **b**  $T_{Ni\tilde{u}o-3}^*$  and **c** zonal SST gradient index ( $^{\circ}C$ , right axis) in CESM-LE ensemble. The black thick lines denote the 40-member ensemble

mean. The shading shows the minimum number of ensemble members (left axis) needed to detect a 95% significant change relative to 1950–1999. **d–f** As in **a–c** but for CMIP5 multimodel ensemble

this part of uncertainty in ENSO amplitude change. We find a considerable inter-member diversity in ENSO amplitude response among CESM-LE members despite relatively small variations of warming pattern. The change in ENSO variance is associated with ocean mean warming in the tropical Pacific. Specifically, a dipole-like inter-member EOF mode

of warming pattern is highly correlated with member diversity in ENSO amplitude response: a member with intensified (weakened) ENSO variability shows a more (less) east–west warming gradient along the equator. This dipole-like pattern looks similar to the second TPDV mode associated with ENSO amplitude modulation in an 1100-year CESM1

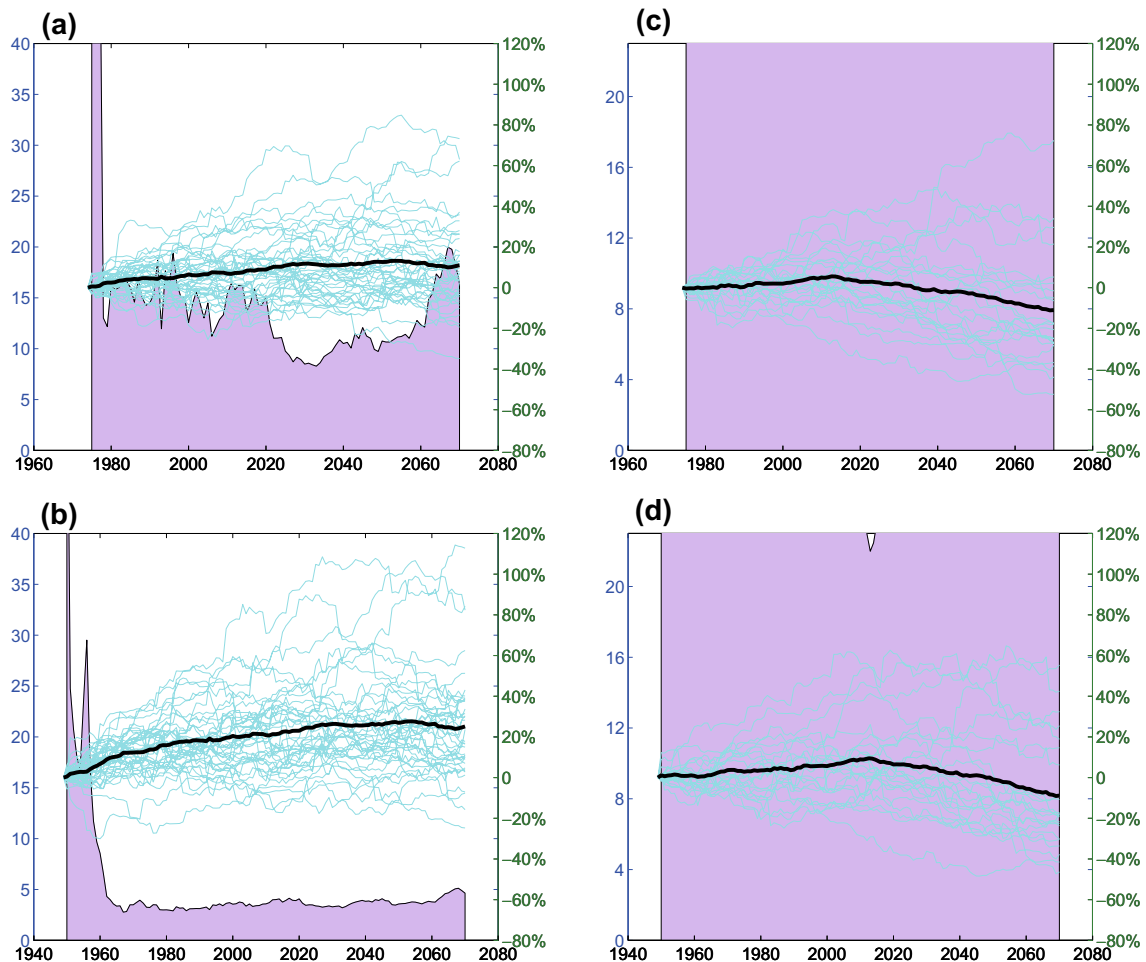


**Fig. 15** Percentage change (*right axis*) of 50-year running standard deviation of the NDJ Niño-3 SST relative to **a** 1950–1999 and **b** 1925–1974 in CESM-LE ensemble. The *black thick lines* denote the 40-member ensemble mean. The *shading* shows the minimum num-

ber (*left axis*) of ensemble members needed to detect a 95% significant change relative to 1950–1999 and 1925–1974, respectively. **c, d** As in **a, b**, but for CMIP5 multimodel ensemble

control run. Next we compare ENSO response in CESM-LE with that in CMIP5 ensemble. The standard deviation of inter-member variability in CESM-LE reaches 80% of that in CMIP5, indicating large contribution of internal variability. Significance detection shows that a large number (~15) of ensemble member is needed to detect a significant change and suppress interference of internal variability in CESM-LE. Furthermore, we suggest that the causations between ocean mean warming and ENSO amplitude change are distinct in CESM-LE and CMIP5 ensemble. Particularly, in CESM-LE, the ENSO amplitude changes rectify onto the mean state, leading to the dipole-like inter-member mode of ocean mean warming in the tropical Pacific.

Abundant previous studies used coupled models with a single ensemble member to investigate ENSO amplitude change under global warming (Watanabe et al. 2012; Cai et al. 2014; Rashid et al. 2016; Ham and Kug 2016; Zheng

et al. 2016). Most of them suggested that the intermodel diversity results from mean state simulation or mean state change but only with a moderate correlation (e.g. Watanabe et al. 2012; Zheng et al. 2016). However, in these studies, uncertainty in ENSO amplitude change among models with single ensemble member is attributed not only by model differences but also by internal variability. Indeed, the responses of ENSO amplitude to global warming in individual models can only be detected with a relatively large number of realizations (Fig. 15). Therefore, to have a better understanding of intermodel diversity in ENSO change under global warming, large ensemble mean in an individual model instead of single member should be used on multimodel comparison. In addition to amplitude, the effect of internal variability to changes in other ENSO properties such as period, flavors, asymmetry, teleconnection should be investigated in the future.

**Acknowledgements** We acknowledge the CESM-LE project for providing model outputs, which may be obtained from <http://www.cesm.ucar.edu/projects/community-projects/LENS/data-sets.html>. We also acknowledge the World Climate Research Programme's Working Group on Coupled Modelling, which is responsible for CMIP, and we thank the climate modeling groups (listed in Table 1 of this paper) for producing and making available their model output. We thank Shang-Ping Xie and Qinyu Liu for helpful discussions. This work was supported by the National Basic Research Program of China (2012CB955600 and 2015CB954300), the National Natural Science Foundation of China (41476003), NSFC-Shandong Joint Fund for Marine Science Research Centers (U1406401), and the China Meteorological Public Welfare Scientific Research Project (GYHY201306027).

## Appendix: The estimation of the minimum ensemble size $N_{min}$

In this study, we evaluate the 95% statistical significance of the ensemble mean changes against a null hypothesis of zero using a one-sample  $t$  test. We use the statistic for ensemble mean defined as

$$t(N-1) = \frac{\bar{x}}{\sigma / \sqrt{N}}$$

where  $\bar{x}$  is the ensemble mean change of ENSO amplitude in a specific 50-year running window relative to that in the first window,  $\sigma$  is the sample standard deviation of the changes in CESM-LE (CMIP5),  $N$  is the ensemble size 40 (23), and  $t(N-1)$  is the  $t$  statistic for the degrees of freedom  $N-1$ . When  $\bar{x}$  and  $\sigma$  satisfy the following relationship

$$\left| \frac{\bar{x}}{\sigma} \right| > \frac{t(N-1)_{p=0.05}}{\sqrt{N}}$$

we can reject the hypothesis and the ensemble mean changes are significant at the 95% confidence level.

According to  $t$ -distribution,  $t(N-1)_{p=0.05} \sim 2$  for 2-sided  $t$  test ( $\sim 1.7$  for 1-sided  $t$  test) when  $N > \sim 20$ . Therefore, we can estimate the minimum ensemble size as  $N_{min} \sim \frac{4}{(\bar{x}/\sigma)^2}$  ( $N_{min} \sim \frac{2.9}{(\bar{x}/\sigma)^2}$ ) for 2-sided (1-sided)  $t$  test. In this study, we detect the significance of changes in  $T_{Ni\tilde{n}o-3}$  based on 1-sided  $t$  test, while detect the significances of  $\Delta T_{Ni\tilde{n}o-3}^*$  and ENSO amplitude changes based on 2-sided  $t$  test.

## References

- An S-I, Choi J (2015) Why the twenty-first century tropical Pacific trend pattern cannot significantly influence ENSO amplitude? *Clim Dyn* 44:133–146
- Bjerknes J (1969) Atmospheric teleconnections from the equatorial Pacific. *Mon Weather Rev* 97:163–172
- Burgman RJ, Schopf PS, Kirtman BP (2008) Decadal modulation of ENSO in a hybrid coupled model. *J Clim* 21:5482–5500
- Cai W, Borlace S, Lengaigne M, Rensch P, Collins M, Vecchi G, Timmermann A, Santoso A, McPhaden M, Wu L, England M, Wang G-J, Guilyardi E, Jin F-F (2014) Increasing frequency of extreme El Niño events due to greenhouse warming. *Nat Clim Change* 4:111–116
- Cai W et al (2015a) ENSO and greenhouse warming. *Nat Clim Change* 5:849–859
- Cai W, Wang G, Santoso A, McPhaden M, Wu L, Jin F-F, Timmermann A, Collins M, Vecchi G, Lengaigne M, England M, Dommenget D, Takahashi K, Guilyardi E (2015b) More frequent extreme La Niña events under greenhouse warming. *Nat Clim Change* 5:132–137
- Choi J, An SI, Yeh SW, Yu J-Y (2013) ENSO-like and ENSO-induced tropical pacific decadal variability in CGCMs. *J Clim* 26:1485–1501
- Chowdary JS, Xie S-P, Tokinaga H, Okumura YM, Kubota H, Johnson NC, Zheng XT (2012) Inter-decadal variations in ENSO teleconnection to the Indo-western Pacific for 1870–2007. *J Clim* 25:1722–1744
- Collins M, An S-I, Cai W, Ganachaud A, Guilyardi E, Jin F-F, Jochum M, Lengaigne M, Power S, Timmermann A, Vecchi G, Wittenberg A (2010) The impact of global warming on the tropical Pacific Ocean and El Niño. *Nat Geosci* 3:391–397
- Deser C, Phillips AS, Bourdette V, Teng H (2012a) Uncertainty in climate change projections: the role of internal variability. *Clim Dyn* 38:527–546
- Deser C, Knutti R, Solomon S, Phillips AS (2012b) Communication of the role of natural variability in future North American climate. *Nat Clim Change* 2:775–779
- DiNezio PN, Kirtman BP, Clement AS, Lee S-K, Vecchi GA, Wittenberg A (2012) Mean climate controls on the simulated response of ENSO to increasing greenhouse gases. *J Clim* 25:7399–7420
- Fang Y, Chiang JCH, Chang P (2008) Variation of mean sea surface temperature and modulation of El Niño–Southern Oscillation variance during the past 150 years. *Geophys Res Lett* 35:L14709. doi:10.1029/2008GL033761
- Guilyardi E, Wittenberg A, Fedorov A, Collins M, Wang C, Capotondi A, van Oldenborgh GJ, Stockdale T (2009) Understanding El Niño in ocean–atmosphere general circulation models: progress and challenges. *Bull Am Meteor Soc* 90:325–340
- Ham YG, Kug J-S (2016) ENSO amplitude changes due to greenhouse warming in CMIP5: role of mean tropical precipitation in the twentieth century. *Geophys Res Lett*. doi:10.1002/2015gl066864
- Hawkins E, Sutton R (2009) The potential to narrow uncertainty in regional climate predictions. *Bull Am Meteor Soc* 90:1095–1107
- Hawkins E, Sutton R (2012) Time of emergence of climate signals. *Geophys Res Lett* 39:L01702
- Hurrell J et al (2013) The community earth system model: a framework for collaborative research. *Bull Am Meteorol Soc* 94:1339–1360
- Johnson NC, Xie S-P (2010) Changes in the sea surface temperature threshold for tropical convection. *Nat Geosci* 3:842–845
- Kay JE et al (2015) The community earth system model (CESM) large ensemble project: a community resource for studying climate change in the presence of internal climate variability. *Bull Am Meteorol Soc* 96:1333–1349
- Kim S-T, Cai W, Jin F-F, Santoso A, Wu L, Guilyardi E, An S-I (2014) Response of El Niño sea surface temperature variability to greenhouse warming. *Nat Clim Change* 4:786–790
- Li J, Xie S-P, Cook ER, Huang G, D'Arrigo R, Liu F, Ma J, Zheng X-T (2011) Interdecadal modulation of El Niño amplitude during the past millennium. *Nat Clim Change* 1:114–118
- Li J, Xie S-P, Cook ER, Morales M, Christie D, Johnson NC, Chen F, D'Arrigo R, Fowler A, Gou X, Fang K (2013) El Niño modulations over the past seven centuries. *Nat Clim Change* 3:822–826



- Liu Z, Vavrus S, He F, Wen N, Zhong Y (2005) Rethinking tropical ocean response to global warming: the enhanced equatorial warming. *J Clim* 18:4684–4700
- Liu F, Luo Y, Lu Y, Wan X (2016) Response of the tropical Pacific Ocean to El Niño versus global warming. *Clim Dyn* 48:935–956
- Lu J, Zhao B (2012) The role of oceanic feedback in the climate response to doubling CO<sub>2</sub>. *J Clim* 25:7544–7563
- Luo Y, Lu J, Liu F, Liu W (2015) Understanding the El Niño-like oceanic response in the tropical Pacific to global warming. *Clim Dyn* 45:1945–1964
- Neale RB et al. (2012) Description of the NCAR community atmosphere model (CAM 5.0). NCAR tech note TN-486, pp 274
- Ogata T, Xie S-P, Wittenberg A, Sun D-Z (2013) Interdecadal amplitude modulation of El Niño/Southern Oscillation and its impacts on tropical Pacific decadal variability. *J Clim* 26:7280–7297
- Philander SG (1990) *El Niño, La Niña and the southern oscillation*. Academic Press, San Diego, CA, 293 pp
- Power S, Delage F, Chung C, Kociuba G, Keay K (2013) Robust twenty-first-century projections of El Niño and related precipitation variability. *Nature* 502:541–545
- Rashid HA, Hirst AC, Marsland SJ (2016) An atmospheric mechanism for ENSO amplitude changes under an abrupt quadrupling of CO<sub>2</sub> concentration in CMIP5 models. *Geophys Res Lett* 43:1687–1694. doi:10.1002/2015GL066768
- Rodgers KB, Friederichs P, Latif M (2004) Tropical Pacific decadal variability and its relation to decadal modulations of ENSO. *J Clim* 17:3761–3774
- Smith TM, Reynolds RW, Peterson TC, Lawrimore J (2008) Improvements to NOAA's historical merged land–ocean surface temperature analysis (1880–2006). *J Clim* 21:2283–2296
- Smith RD et al (2010) The parallel ocean program (POP) reference manual: ocean component of the community climate system model (CCSM) and community earth system model (CESM). Los Alamos National Laboratory Tech Rep LAUR-10-01853, p 141
- Stevenson SL (2012) Significant changes to ENSO strength and impacts in the twenty-first century: results from CMIP5. *Geophys Res Lett* 39:L17703
- Sun F, Yu J-Y (2009) A 10–15-yr modulation cycle of ENSO intensity. *J Clim* 22:1718–1735
- Taylor KE, Stouffer RJ, Meehl GA (2012) An overview of CMIP5 and the experiment design. *Bull Am Meteorol Soc* 93:485–498
- Vecchi GA, Soden BJ (2007) Global warming and the weakening of the tropical circulation. *J Clim* 20:4316–4340
- Watanabe M, Wittenberg AT (2012) A method for disentangling El Niño–mean state interaction. *Geophys Res Lett* 39:L14702. doi:10.1029/2012GL052013
- Watanabe M, Kug J-S, Jin F-F, Collins M, Ohba M, Wittenberg AT (2012) Uncertainty in the ENSO amplitude change from the past to the future. *Geophys Res Lett* 39:L20703
- Wittenberg AT (2002) ENSO response to altered climates. Ph.D. thesis, Princeton University
- Wittenberg AT (2009) Are historical records sufficient to constrain ENSO simulations? *Geophys Res Lett* 36:L12702
- Wittenberg AT, Rosati A, Delworth TL, Vecchi GA, Zeng F (2014) ENSO modulation: is it decadal predictability? *J Clim* 27:2667–2681
- Xie S-P, Deser C, Vecchi GA, Ma J, Teng H, Wittenberg AT (2010a) Global warming pattern formation: sea surface temperature and rainfall. *J Clim* 23:966–986
- Xie S-P, Du Y, Huang G, Zheng X-T, Tokinaga H, Hu K, Liu Q (2010b) Decadal shift in El Niño influences on Indo-western Pacific and East Asian climate in the 1970s. *J Clim* 23:3352–3368
- Yeh S-W, Kirtman B (2004) Tropical Pacific decadal variability and ENSO amplitude modulation in a CGCM. *J Geophys Res* 109:C11009. doi:10.1029/2004JC002442
- Yeh S-W, Kirtman B (2007) ENSO amplitude changes due to climate change projections in different coupled models. *J Clim* 20:203–217
- Zheng X-T, Xie S-P, Lv L-H, Zhou Z-Q (2016) Intermodel uncertainty in ENSO amplitude change tied to Pacific ocean warming pattern. *J Clim* 29:7265–7279
- Zhou Z-Q, Xie S-P, Zheng X-T, Liu Q, Wang H (2014) Global warming-induced changes in El Niño teleconnections over the North Pacific and North America. *J Clim* 27:9050–9064